12th International Conference on Fracture Mechanics of Concrete and Concrete Structures
FraMCoS-12
B.L.A. Pichler, Ch. Hellmich, P. Preinstorfer (Eds)

https://doi.org/10.21012/FC12.1279
MS13-3:3

RELIABILITY ASSESSMENT OF HISTORICAL REINFORCED CONCRETE BRIDGE PIERS BASED ON NONLINEAR FRACTURE MECHANICS MODELING AND SAFETY FORMATS

DRAHOMÍR NOVÁK[*], LUKÁŠ NOVÁK[*], DAVID LEHKÝ[*],

ALFRED STRAUSS[†] AND BENJAMIN TÄUBLING-FRULEUX[†]

[*] Brno University of Technology, Faculty of Civil Engineering, Institute of Structural Mechanics
Veveří 95, 602 00 Brno, Czech Republic
e-mail: drahomir.novak@vut.cz, https://www.fce.vutbr.cz

[†] BOKU University, Department Land, Water and Infrastructures
Peter Jordan Strasse 82, 1190 Vienna, Austria
e-mail: alfred.strauss@boku.ac.at, https://boku.ac.at/baunat/iki

Key words: Nonlinear fracture mechanics, Reinforced concrete, Strengthening, Reliability, Safety formats.

Abstract: Many existing concrete structures have been fulfilling their purpose for several decades, but they may no longer meet current structural safety standards due to various factors. This fact highlights the urgent need for innovative solutions to ensure the durability and performance of these structures under increasing load and changing environment. Statistical study has to be included to consider uncertainties, also safety formats approaches can be utilized. The aim of this research is to show how a procedure for quality control and safety assessment of 100 m high concrete piers was developed based on non-linear finite element analysis and digital twin technology considering uncertainties involved. Piers are parts of Jauntal bridge, a 60-year-old, 450 m long railway bridge that has been equipped with a new bridge deck. The purpose of the study was to investigate structural safety, serviceability, durability, and remaining service life of the bearing socket and pier systems equipped with a new confinement concept. The research uses a reliability-based approach utilizing advanced probabilistic methods, based on reliability index determination and efficient safety format approaches. Standard ECoV and Eigen ECoV methods were employed for an estimation of mean values and standard deviations for all steps of the finite element analysis, assuming two limit cases of probability distribution of resistance – Gaussian and Lognormal. The stochastic model contains only the 4 most significant random variables of the computational model representing the material characteristics of the concrete pier.

1 INTRODUCTION

The text discusses the need for innovative solutions to ensure the safety and reliability of aging concrete structures, such as bridges and tunnels, which may no longer meet current structural safety standards. The process involves incorporating monitoring data into structural assessments to ensure safety, serviceability, durability, and the remaining service life of these structures.

A specific case is presented where a safety assessment procedure was developed for a 450 m long bridge mounted on 60-year-old, 100 m high concrete piers. The assessment aimed to

ensure the structural integrity of the bridge by strengthening the piers using a confinement concept. The research also highlights the potential of digitalization to enhance infrastructure resilience [1], [2]. This is achieved by developing a Nonlinear Finite Element Analysis (NLFEA)-based digital twin, which links photogrammetric observations (e.g., deformations on the real structure) with structural assessments. The combination allows for the assessment of structural safety through the application of the classical limit state function concept, including the Serviceability Limit State (SLS) and Ultimate Limit State (ULS), under realistic conditions. ECoV safety formats are used to address the material uncertainties associated with aged concrete piers.

2 PIER HEAD OF JAUNTAL BRIDGE

The Jauntal bridge, located 96 meters above the Drau Valley in Carinthia, Austria, is one of the highest railway bridges in Europe. Originally built in 1961, the bridge has a total length of approximately 430 meters. Recently, the original steel box girder superstructure was replaced with a new structure that includes a double-track and a pedestrian and cycle path underneath. The renewed bridge was opened for traffic in late 2023.

A comprehensive monitoring system has been installed on the bridge to monitor both the construction and operational phases, enabling a thorough performance evaluation. The pier heads are a critical component of the structure, as the loads imposed upon them have increased significantly. To reinforce the pier heads, prestressing tendons were utilized, providing confinement and enhancing their load-bearing capacity.

Particular attention was paid to the shear forces in the pier heads to enable a three-dimensional stress state, thereby increasing the load-bearing capacity. The maximum vertical force acting on the bearing socket block through the structure, as determined by the new static analysis, is 50 MN. This load was also defined by the owner and the static design office as the critical load for the design level, at which a maximum crack width of 0.1 mm may occur in the old pier head.

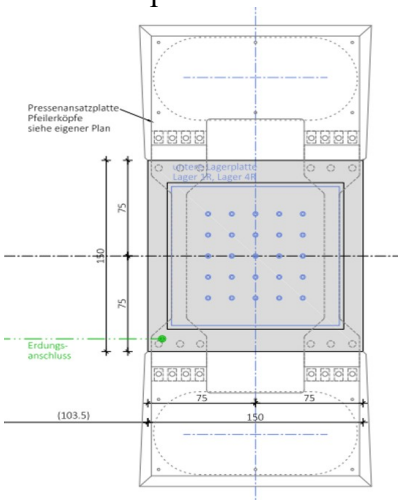

Figure 1: Ground plan of the right pier head.

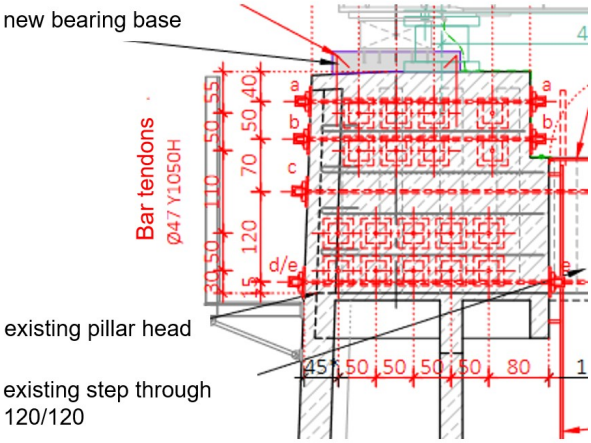

Figure 2: Prestressing of the left pier head by tendons.

3 COMPUTATIONAL MODELLING

The aim of this modelling was to simulate the complex interactions between a prestressed old pier head and a newly installed bearing base on the old pier head. In particular, the goal is to assess whether the new, higher vertical load caused by the passage of the train and the new composite structure can be transferred. Several prestressing situations were analyzed and extensive tests were carried out to determine the material properties of the real concrete [3]. These properties were adopted to the real properties of the old concrete using innovative latest test methods. ATENA Scientific software package [4] was used to model the complex behavior of the 3D

column head area, as shown in Figure 3. The model, reduced with respect to the symmetry plane, consists of 5321 brick elements and 52,467 degrees of freedom (DOF). The total nonlinear analysis up to a maximum cracking of 0.05 m takes 7.42 hours. Several phases were modeled; In this scenario, prestressing is applied symmetrically and simultaneously up to a prestressing level of 80% before any loads from traffic and the supporting structure are applied to the pier. This means that the prestressing force is introduced to the structure to a significant extent (80% of the total prestressing force) before it is subjected to additional loads. The cracking of the structure occurs only due to a load increase from the structure and the traffic, not from the prestressing itself. This implies that prestressing is effective in counteracting the initial stresses and that the additional loads are the primary cause of any potential cracking.

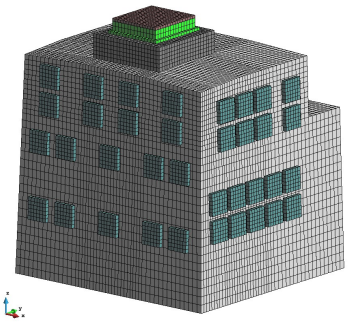

Figure 3: FE model of the pier head with tendons

For the non-linear finite element modelling in the Scientific ATENA Tool and the development of the digital twin, the concrete models determined by tests were used, which roughly correspond to the strength class C40/50 according to ÖNORM EN 1992-1-1 [5] for the new bearing bases. The characteristic cylindrical compressive strength of f_{ck} = 29 MPa according to the functional relationships of CEB-fib Model Code 90 [6], which are shown in Table 1, was used for the material properties of the old concrete of the pier heads. Stress-strain behavior and the crack development of the cylinder tests were also used for calibration. The prestressing bars used in these model analyses had a diameter of 47 mm and were modeled according to the bilinear stress-strain law with the parameters given in Table 2. The prestressing force, including the direct prestressing force losses, was P=1275 kN per bar. For the sake of simplicity, no bond between the bars and the concrete was assumed in these analyses. The load-deflection curves in Figure 4 illustrate the behavior of three different models: one without reinforcement, one with non-prestressed reinforcement, and one with prestressing. These curves highlight how each model responds to applied loads, showing the relationship between the load and the resulting deflection. Figure 5 presents the dependence of load application vs. crack width. This relationship is crucial for understanding the structural integrity and performance of the models under different loading conditions. The crack width is a key indicator of potential failure or damage, and its correlation with the applied load helps in assessing the reliability and safety of the structures.

Table 1: Material parameters of old concrete

Material parameter	Value	Unit
Modulus of elasticity E	33253.6	MPa
Compressive strength f_c	37.0	MPa
Tensile strength f_{ct}	2.83	MPa
Poisson‘s ratio μ	0.2	–
Fracture energy G_f	0.00014	MN/m
Plastic strain at f_c ε_{cp}	0.00133	–
Onset of crushing f_{c0}	5.95	MPa
Critical comp. displ. w_d	0.0005	m

Table 2: Material parameters of prestressing rods

Parameter	Value	Unit
Modulus of elasticity E	200000	MPa
Yield strength f_y	950	MPa
Strain at bar rupture ε_u	0.025	-
Stress at bar rupture f_u	1050	MPa

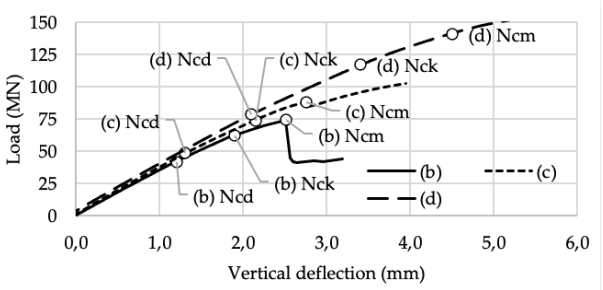

Figure 4: Load–deformation diagram: (b) modelling. without reinforcement, (c) with non-prestressed reinforcement, (d) with prestressing.

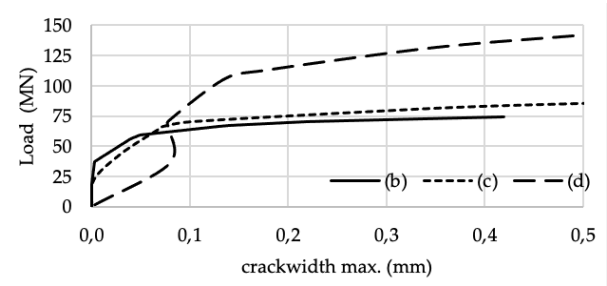

Figure 5: Load vs max. crack width diagram: (b) modelling without reinforcement, (c) with non-prestressed reinforcement, (d) with prestressing.

4 SAFETY FORMATS

4.1 Theoretical principles

The basic reliability concept is given by the well-known formula $Z = R - E$ where Z is a random variable representing the safety margin, defined as the difference between structural resistance R and action effect E. The probability of the negative safety margin (probability of failure) is used in a fully probabilistic method to quantify the structural safety. The semi-probabilistic approaches assume the separation of these two random variables, structural resistance R and action effect E, using their design values instead of the complete probability distributions. Design value of resistance is generally defined as:

$$R_d = F_R^{-1}(-\alpha_R \beta), \tag{1}$$

where F_R^{-1} represents inverse cumulative distribution function of R, α_R is a sensitivity factor and β is the target reliability index (both can be found in Eurocodes reflecting the type of the structure). This section is focused on the estimation of R_d using standard values $\alpha_R = 0.8$ and β=3.8. The R is a result of a function $r(\mathbf{X})$ of input random vector ($\mathbf{X}$ being a vector of N random variables) represented by costly FEM computational model. The probability distribution of R is described by distribution function, its mean value and coefficient of Variation (CoV). Gaussian and Lognormal distributions are typically assumed in Eurocodes and therefore, the complex reliability analysis reduces to the estimation of the first two statistical moments. There are various methods for estimating of the first two statistical moments (see [7] for a comparison) often referenced as Estimation of Coefficient of Variation (ECoV) methods.

Standard ECoV method often used in analyses of concrete structural members was developed by Červenka [8] and later implemented into the *fib* Model Code 2010 [9]. It is based on a simplified formula for the estimation of a characteristic value of a Lognormal variable with the mean value μ_R and CoV v_R using only two numerical simulations R_m (with mean values of input variables) and R_k (using characteristic values of input variables). The formula of the standard ECoV method is:

$$v_R = \frac{1}{1.645} ln\left(\frac{R_m}{R_k}\right) \tag{2}$$

In this paper, we will investigate also the influence of the assumed Lognormal distribution and thus the following Gaussian transformation of the formula will be also employed in the numerical analysis:

$$v_R = \frac{R_m - R_k}{1.645 R_m} \tag{3}$$

(1) (1)

The recently proposed Eigen ECoV [10] is based on the idea of projecting input random vector on 1D eigen distribution Θ with variance equal to the first eigenvalue of input covariance matrix $\sigma_\Theta^2 = \sum \sigma_{X_i}^2 = \lambda_1$ and mean value is simply obtained as:

$$\mu_\Theta = \sqrt{\sum_{i=1}^{N} \left(\mu_{X_i}\right)^2} \tag{4}$$

The Eigen ECoV method can be seen as a generalization of the standard ECoV independent on the assumed two-parametric distribution. In the original proposal, there are three levels of Eigen ECoV differing in differencing schemes and associated

computational cost (number of numerical simulations). The most promising Eigen ECoV formula for the estimation of v_R offering a balance between efficiency and accuracy is:

$$v_R \approx \frac{3R_m - 4R_{\Theta\frac{\Delta}{2}} + R_{\Theta\Delta}}{\Delta_\Theta} \cdot \frac{\sqrt{\lambda_1}}{R_m} \tag{5}$$

where simulation $R_{\Theta\Delta} = r(X_{\Theta\Delta})$ is calculated with coordinates of input realization $X_{\Theta\Delta} = (X_{1\Delta}, \dots, X_{N\Delta})$ and $R_{\Theta\frac{\Delta}{2}} = r\left(X_{\Theta\frac{\Delta}{2}}\right)$ with coordinates $X_{\Theta\frac{\Delta}{2}} = \left(X_{1\frac{\Delta}{2}}, \dots, X_{N\frac{\Delta}{2}}\right)$. The input vectors consisting of reduced values of input random variables are $X_{i\Delta} = F_i^{-1}(\Phi(-c))$ and the intermediate coordinates are as follows:

$$X_{i\frac{\Delta}{2}} = \mu_{X_i} - \frac{\mu_{X_i} - X_{i\Delta}}{2} = \frac{\mu_{X_i} + X_{i\Delta}}{2} \tag{6}$$

Δ_Θ represents the distance between μ_Θ and desired quantile $F_\Theta^{-1}(\Phi(-c))$ obtained under the assumption of Gaussian distribution as $\Delta_\Theta = c \cdot \sqrt{\lambda_1}$ and for comparison, under assumption of lognormal distribution as $\Delta_\Theta = \mu_\Theta - \mu_\Theta \cdot exp\left(-c\frac{\sqrt{\lambda_1}}{\mu_\Theta}\right)$. For proper comparison, we use $c = 1.645$ leading to $X_{ik} = X_{i\Delta}$, and thus the simulation with reduced input variables coincides with R_k used in standard ECoV.

4.2 Stochastic model

Standard ECoV and Eigen ECoV methods were employed for an estimation of mean values and standard deviations for all steps of the finite element analysis assuming two limit cases of probability distribution of resistance – Gaussian and Lognormal. The stochastic model contains only 4 the most significant random variables of computational model representing concrete material characteristics, see Table 3.

Table 3: Material properties of existing pier concrete

Material parameters	Mean μ	CoV v_R	X_{ik}	$X_{i,\Delta/2}$
Modulus of elasticity E	33253.6	0.16	25601	29427
Compressive strength f_c	37.0	0.12	30.4	33.7
Tensile strength f_{ct}	2.83	0.16	2.18	2.50
Fracture energy G_f	14×10^{-5}	0.21	9.95×10^{-5}	12×10^{-5}

4.3 Probabilistic results

Note that obtained results for each of the methods are based on a different number of simulations (calculations of computational model): Standard ECoV – 2, Eigen ECoV – 3 (one additional simulation to standard ECoV). However, in our case we use step-size $c = 1.645$ and thus it is possible to use identical simulations for both methods (simulation with mean and characteristic values) extended by one intermediate additional simulation for Eigen ECoV.

Summary of the results obtained can be seen in Fig. 6. The left column shows change of mean values and ±σ intervals with increasing load steps for both investigated quantities of interest: reactions R (Fig. 6a) and crack width w (Fig. 6b). The right column shows the evolution of standard deviations with increasing load step for better comparison of both safety format methods and both assumed probability distributions. It can be observed that differences between both methods are negligible in most cases for reactions, except standard deviations in post-peak phase. This is caused by significant non-linearity of the material model in the final phase of load-displacement diagram. However, as can be seen in Fig. 6c, it does not significantly affect the estimation of quantiles (±σ), since both methods have opposite trend of underestimation/overestimation of variance for reactions and crack widths, and thus both methods lead to very similar quantiles in graph Fig. 6c. Note that in Fig. 6c, the horizontal axis shows mean value of crack width in each load step. Similarly, design values of

resistance estimated for limit crack width 0.5 mm and target β=3.8 by both methods are almost identical as can be seen in Fig 6d. Similarly, assumptions of Gaussian or Lognormal distributions of resistance don't lead to significant differences in the estimated design values and thus it is possible to further use only results for lognormal distributions.

The final study presented in Fig. 7 shows relationships between crack width and load with respect to structural safety. Specifically, Fig. 7a extends the results from Fig 6d for several values of β and target mean values of crack width in range of 0.2 to 0.5 mm. From this figure it is ovious, that there are negligible differences between both standard ECoV and Eigen ECoV methods. On the other hand, one can reformulate the problem. Since each load step in FEM is represented by a deformation increment, both reactions and crack widths for each load step are random variables. In Fig. 7a, the target quantity is the standard design load R_d such that the mean value of a crack width $\mathbb{E}[w]$ doesn't exceed the given threshold t with target probability P_β, i.e.:

$$R_d = R \mid P\{(\mathbb{E}[w(R)] > t)\} \leq P_\beta \quad (7)$$

However, one can be also interested in the mean load $\mathbb{E}[R]$ associated to the target design crack width, i.e.:

$$R_{d,w} = \mathbb{E}[R] \mid P\{(w(\mathbb{E}[R]) > t)\} \leq P_\beta \quad (8)$$

The difference between both formulations lies in the applied mean estimators for each load step – mean crack width for Eq. 7 and mean load for Eq. 8 respectively. The former is a standard definition of the design load, while the latter could be important for serviceability limit state emphasizing the uncertainty of the crack width. As can be seen in Fig. 7a, the difference between standard ECoV and Eigen ECoV for standard design load is negligible. On the other hand, the estimation of the mean load associated with target design crack width compared in Fig. 7b shows some discrepancy in both methods. The difference between methods is caused by a difference in variance estimations of crack widths in each load step also depicted in Fig. 6b. However, it is worthy to note that absolute differences in loads are less than 1%. Note that for proper comparison with design values to normative approach, it is necessary to reduce the obtained values by an additional factor $\gamma_{R_d} = 1.15$ reflecting also the model uncertainty [9]. Note that final study of influence of uncertainties of old concrete parameters represents two alternative formulations – Mean crack width vs. Design load (Fig. 7a) and Design crack width vs. Mean load (Fig. 7b) for several values of β.

5. CONCLUSION

On the basis of the case study of the railway Jauntal bridge in Carinthia, Austria, decision processes and evaluation models could be developed between the scientific partner and the supervising engineering office as well as the operator for the real problem of evaluating the load-bearing capacity of the reinforced piers with the help of in-depth non-linear methods.

As a result, the real digital twin of the pier head was perfectly modelled and it was shown that the interaction with the existing concrete can withstand a maximum load of 141 MN with a maximum crack width of 0.5 mm, which is above the design loads of 50 MN. In addition to the deterministic nonlinear fracture mechanics modelling, it was also of paramount importance to predict the variability of the responses and crack width based on the uncertainties of the basic material random variables the safety level using the standard ECOV and Eigen-ECOV techniques. It should be noted that in this case of a computationally very demanding deterministic analysis, a fully probabilistic approach based on Monte Carlo simulation is not possible and the ECOV techniques are the only viable methods.

The estimated design value of the resistance for the 0.5 mm crack width limit is approximately 85 MN (after deduction of γ_{Rd}), which is still significantly higher than the design load determined using the standard partial safety factor method. This means that the design value is on the safe side with considerable reserves, even taking into account

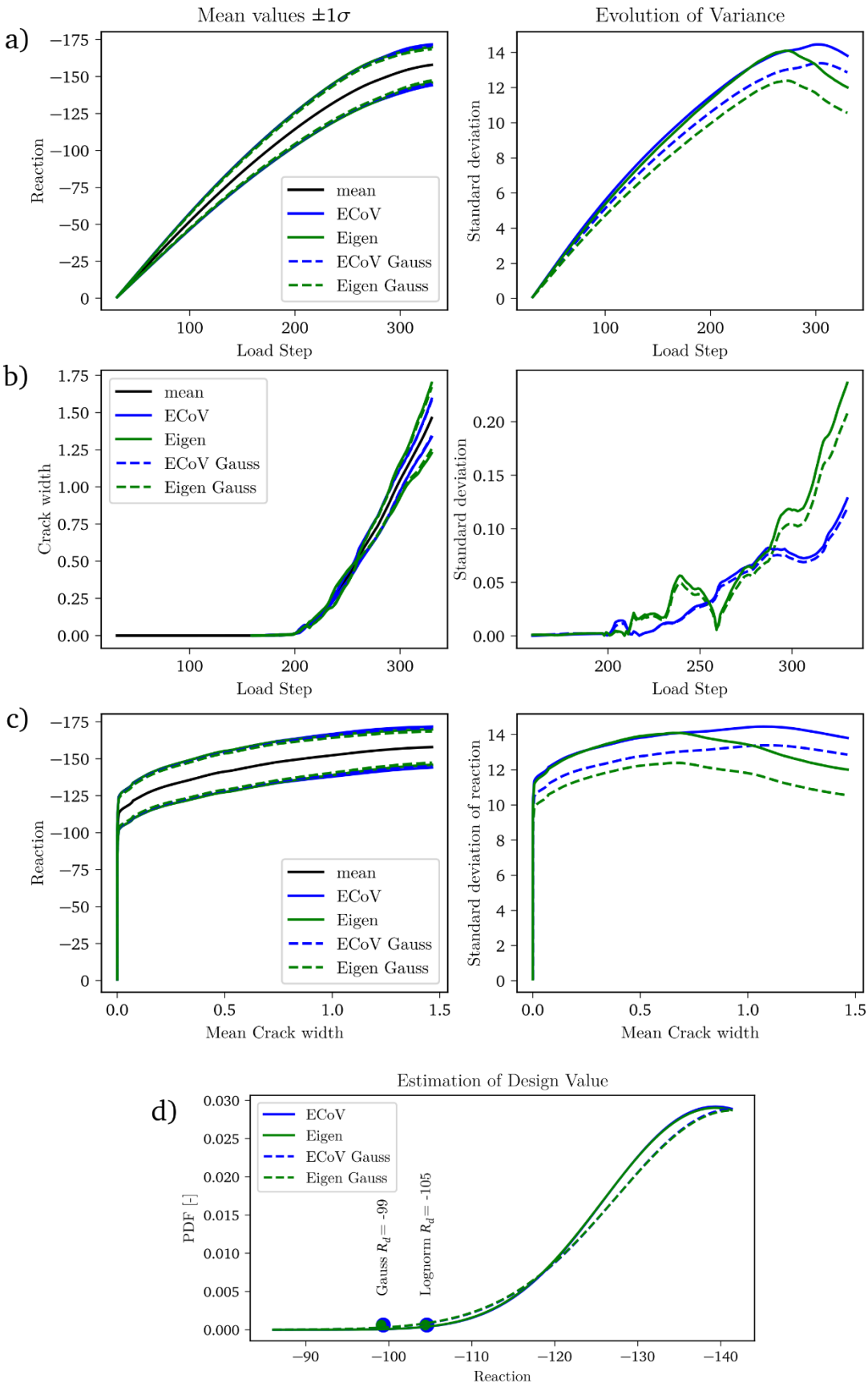

Figure 6: Obtained mean values, standard deviations and ±σ intervals estimated by Eigen ECoV and standard ECoV for: a) Reactions vs Load Step (displacement), b) Crack width vs Load Step (displacement), c) Reactions vs Crack width. Finally, graph d) shows design values of resistance assuming Lognormal and Gaussian distributions of R for limit crack width 0.5mm.

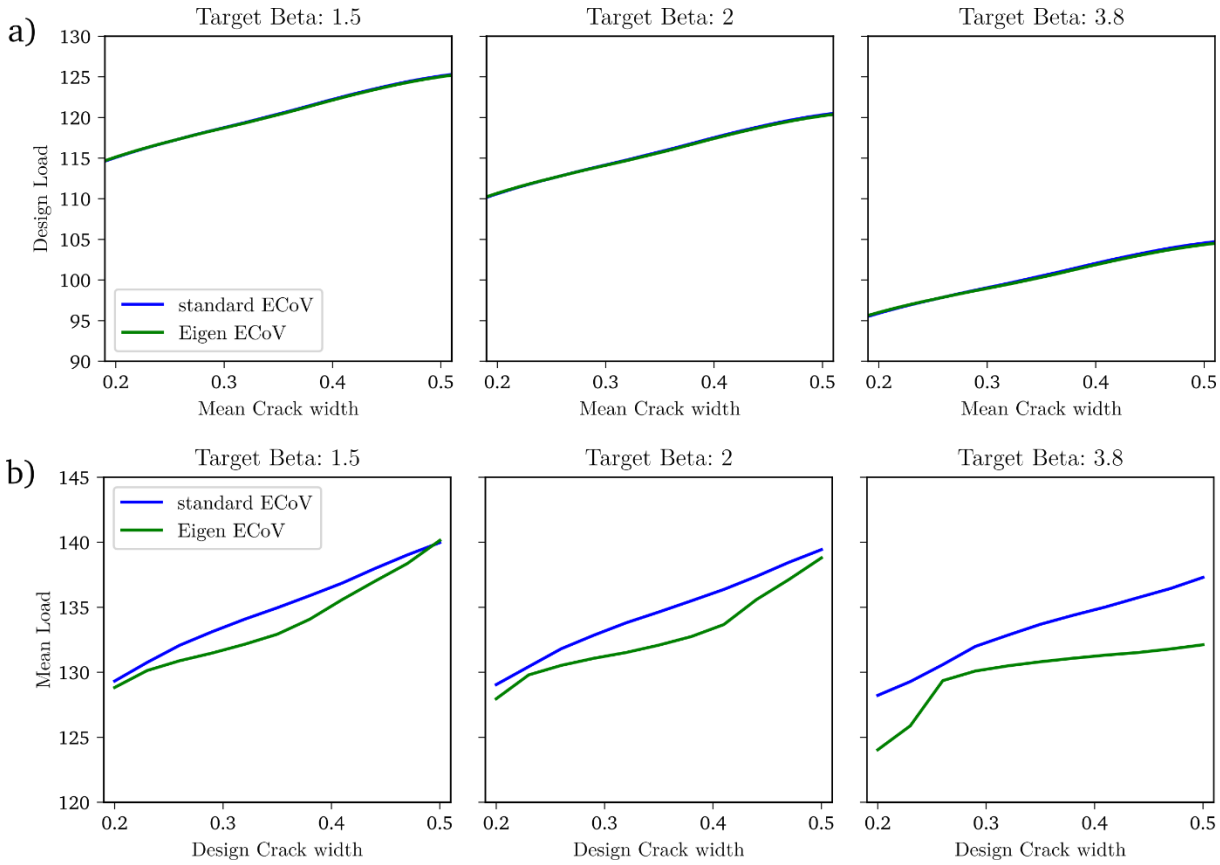

Figure 7: Comparison of a) design loads for a determined mean crack width and reliability index; and b) design crack width for a determined mean load and reliability index.

the dominant material uncertainties. In addition, a comprehensive statistical analysis was carried out with regard to the assumed probability distributions. The final analysis of the influence of uncertainties in the material parameters of the old concrete shows the correlations between crack width and load with regard to structural safety. The results were presented for different values of β and the target mean crack widths in the range of 0.2 to 0.5 mm.

ACKNOWLEDGMENTS

Authors acknowledge the support by European Union within the framework of programme Interreg Austria-Czechia 2021-2027, project No. ATCZ00068 / IREC. Czech authors acknowledge the Czech Science Foundation, project No. 24-10892S and appreciate financial support by European Regional Development Fund (Innovative methods of materials diagnostics and monitoring of engineering infrastructure to increase its durability and service time – INODIN, CZ.02.01.01/00/23_020/0008487).

REFERENCES

[1] Strauss A, Bergmeister K, Daró P, Mancini G, Sattler F, Bigaj-van Vliet A. 2023. Monitoring and data-informed approaches for the assessment of existing structures. *Structural Concrete*. **24**(4): 4433–4445.

[2] Darò, P., Longo, M., Mancini, G., Negri, S., Vliet, A.B.-v. and Allaix, D.L. 2023. Data-informed safety assessment of existing transport infrastructures. *ce/papers*. **6**: 528-536.

[3] ÖBB bereitgestellte Statische Berechnung – Jauntalbrücke
[4] Červenka V., Jendele L., Červenka J. 2016. ATENA Program Documentation Part 1, Theory
[5] Austrian Standards International (ASI). 2018. ÖNORM EN 1992-1-1: Eurocode 2: Design of concrete structures – Part 1-1: General rules and rules for buildings.
[6] fib Fédération internationale du béton. 1993. CEB-FIP Model Code 1990: Design Code
[7] Novák, L., Červenka, J., Červenka, V., Novák, D. and Sýkora, M. 2023. Comparison of advanced semi-probabilistic methods for design and assessment of concrete structures. *Structural Concrete.* **24** (1).
[8] Červenka V. 2013. Reliability-based non-linear analysis according to fib model code 2010. *Structural Concrete*. **14**: 19-28.
[9] fib 2010. 2013. fib Model Code for concrete structures. Vol 1. Lausanne: Ernst & Sohn.
[10] Novák, L. and Novák, D. 2021 Estimation of coefficient of variation for structural analysis: The correlation interval approach. *Structural Safety*. 2021.